Protein tyrosine phosphatase σ targets apical junction complex proteins in the intestine and regulates epithelial permeability

Ryan Murchie[a,b,c], Cong-Hui Guo[a,b], Avinash Persaud[a,c], Aleixo Muise[a,b,d,1], and Daniela Rotin[a,c,1]

[a]Program in Cell Biology and [b]Inflammatory Bowel Disease Centre, Division of Gastroenterology, Hepatology, and Nutrition, The Hospital for Sick Children, Toronto, ON, Canada, M5G 1X8; and [c]Department of Biochemistry and [d]Institute of Medical Science, University of Toronto, Toronto, ON, Canada M5S 1A8

Edited by Joseph Schlessinger, Yale University School of Medicine, New Haven, CT, and approved November 18, 2013 (received for review August 14, 2013)

Protein tyrosine phosphatase (PTP)σ (*PTPRS*) was shown previously to be associated with susceptibility to inflammatory bowel disease (IBD). PTPσ$^{-/-}$ mice exhibit an IBD-like phenotype in the intestine and show increased susceptibility to acute models of murine colitis. However, the function of PTPσ in the intestine is uncharacterized. Here, we show an intestinal epithelial barrier defect in the PTPσ$^{-/-}$ mouse, demonstrated by a decrease in transepithelial resistance and a leaky intestinal epithelium that was determined by in vivo tracer analysis. Increased tyrosine phosphorylation was observed at the plasma membrane of epithelial cells lining the crypts of the small bowel and colon of the PTPσ$^{-/-}$ mouse, suggesting the presence of PTPσ substrates in these regions. Using mass spectrometry, we identified several putative PTPσ intestinal substrates that were hyper–tyrosine-phosphorylated in the PTPσ$^{-/-}$ mice relative to wild type. Among these were proteins that form or regulate the apical junction complex, including ezrin. We show that ezrin binds to and is dephosphorylated by PTPσ in vitro, suggesting it is a direct PTPσ substrate, and identified ezrin-Y353/Y145 as important sites targeted by PTPσ. Moreover, subcellular localization of the ezrin phosphomimetic Y353E or Y145 mutants were disrupted in colonic Caco-2 cells, similar to ezrin mislocalization in the colon of PTPσ$^{-/-}$ mice following induction of colitis. Our results suggest that PTPσ is a positive regulator of intestinal epithelial barrier, which mediates its effects by modulating epithelial cell adhesion through targeting of apical junction complex-associated proteins (including ezrin), a process impaired in IBD.

Protein tyrosine phosphatase (PTP)σ, encoded by *PTPRS* (1), consists of a cell adhesion molecule-like ectodomain containing three immunoglobulin (Ig)-like and three to eight fibronectin type III repeats, a transmembrane domain, and a cytosolic region with two PTPase domains, of which the first (D1) is catalytically active (2). PTPσ expression is developmentally regulated and found primarily in the nervous system and specific epithelia (3, 4). It was previously shown to play a role in axon growth and path finding (5–7), neuroregeneration (5, 8, 9), autophagy (10), and neuroendocrine development (11–13).

To investigate the function of PTPσ in vivo, our group (11) and Tremblay and coworkers (12) generated PTPσ$^{-/-}$ mice. These mice exhibited high neonatal mortality, various neurological and neuroendocrine defects, colitis, and cachexia (5, 11, 13, 14). Analysis of the intestinal tissue in surviving mice by our group revealed the presence of mucosal inflammation, intestinal crypt branching, and villus blunting: all features of colitis similar to the enteropathy associated with human inflammatory bowel disease (IBD) (15). Notably, PTPσ$^{-/-}$ mice also showed increased susceptibility to chemical and infectious models of murine colitis, specifically treatment with dextran sodium sulfate (DSS) or infection with *Citrobacter rodentium* (15). The intestinal phenotype in the mice strongly inferred a connection between PTPσ and IBD.

IBD is a chronic, idiopathic, relapsing disorder affecting the gastrointestinal tract, where Crohn disease and ulcerative colitis (UC) are the two major forms (16). In IBD pathogenesis, the presence of environmental factors together with polymorphisms in IBD-susceptibility genes cause an abnormal innate and adaptive host immune response to commensal gut bacteria, leading to sustained and deleterious inflammation (17). Chronic infection (18, 19), dysbiosis (19), defective mucosal barrier defense (20), and insufficient microbial clearance (19) have all been implicated as factors contributing to IBD pathogenesis. The disease is known to have a strong genetic component, as evidenced by specific populations exhibiting a disproportionately high incidence (21) and the high disease concordance between monozygotic twins (22). Genome-wide association studies and associated metaanalyses have implicated several genes and pathways in IBD, notably genes associated with intestinal barrier defense [*MYO9B* (23), *PARD3* (24), *MAGI2* (24), *CDH1* (25, 26)].

Through SNP analysis of IBD patients, we showed that *PTPRS* is genetically associated with UC (15). The identified SNP polymorphism leads to alternative splicing in the extracellular region of the epithelial isoform of PTPσ, causing loss of the third Ig domain (15). This splicing might potentially lead to altered ligand recognition or may affect receptor dimerization (27). In addition, through an interaction-trap assay, we identified the apical junction complex (AJC) proteins E-cadherin (*CDH1*) and β-catenin (*CTNNB1*) as colonic substrates of PTPσ (15). Interestingly, recent large-scale genetic studies have identified over 160 loci that affect risk of developing IBD, many of which involved in barrier regulation (24, 28, 29).

The AJC confers polarity to epithelial cells and maintains intestinal barrier integrity (30). Defective regulation of AJC proteins creates disrupted epithelial barriers, permeability defects, and aberrant intestinal morphology (30, 31), similar to defects seen in IBD. The connection between the AJC and IBD is further

Significance

Polymorphisms in the protein tyrosine phosphatase (PTP)σ (*PTPRS*) gene were previously shown to be associated with inflammatory bowel disease (IBD), and PTPσ knockout mice exhibit an intestinal IBD phenotype, but how PTPσ is involved in IBD is unknown. Our studies here show that PTPσ knockout mice exhibit a leaky intestinal epithelium that may explain the observed IBD phenotype. We further identify the junctional protein ezrin as an in vivo intestinal substrate for PTPσ and identify specific tyrosine phosphorylation sites on ezrin that are targeted by PTPσ, leading to removal of ezrin from its plasma membrane localization. These studies help explain the role of PTPσ in IBD.

Author contributions: R.M., A.P., A.M., and D.R. designed research; R.M., C.-H.G., and A.P. performed research; R.M. and A.P. analyzed data; and R.M., A.M., and D.R. wrote the paper.

The authors declare no conflict of interest.

This article is a PNAS Direct Submission.

[1]To whom correspondence may be addressed. E-mail: aleixo.muise@sickkids.ca or drotin@sickkids.ca.

This article contains supporting information online at www.pnas.org/lookup/suppl/doi:10.1073/pnas.1315017111/-/DCSupplemental.

CELL BIOLOGY

demonstrated by our earlier SNP analysis, which revealed a haplotype polymorphism in *CDH1* that is associated with Crohn disease, leading to a truncated E-cadherin protein that fails to localize to the plasma membrane (PM), as also observed in IBD patient biopsy samples (25). Thus, we postulate that PTPσ regulates epithelial barrier integrity through regulation of AJC proteins and that defective PTPσ function may contribute to IBD.

In this report, we demonstrate an intestinal epithelial barrier defect in the PTPσ$^{-/-}$ mice and identify the AJC protein ezrin as an in vivo colonic substrate for PTPσ. We further demonstrate that dephosphorylation of ezrin-Y353 or -Y145 by PTPσ leads to its redistribution from the PM to the cytosol, similar to its localization following induction of IBD in mice.

Results

PTPσ$^{-/-}$ Mice Exhibit Defects in Intestinal Barrier Integrity. Given the importance of the adherens junction in epithelial cell adhesion and barrier defense, we investigated the integrity of the intestinal epithelial layer in our PTPσ$^{-/-}$ mice by evaluating the permeability and electrophysiology of the small bowel and colon ex vivo and performing in vivo tracer studies. Small bowel and colon sections from PTPσ$^{+/+}$ and PTPσ$^{-/-}$ mice were analyzed in an Ussing Chamber. PTPσ$^{-/-}$ mouse colon and small bowel both showed a significant decrease in transepithelial electrical resistance (TEER) (Fig. 1*A*) and increased macromolecular flux (Fig. 1*B*) compared with PTPσ$^{+/+}$ littermates. PTPσ$^{+/-}$ mice were similar to wild-type (WT) controls. These data suggest that loss of PTPσ function leads to loss of epithelial resistance, indicating a potential defect in intestinal permeability. To confirm these observations in vivo, mice were gavaged with fluorescein isothiocyanate (FITC)-conjugated dextran that acts as a molecular probe to evaluate epithelial barrier permeability. Two different size dextran conjugates were used, 4.4 kDa and 40 kDa, to assess both paracellular and macromolecular permeability, respectively. PTPσ$^{-/-}$ mouse small bowel and colon tissue showed

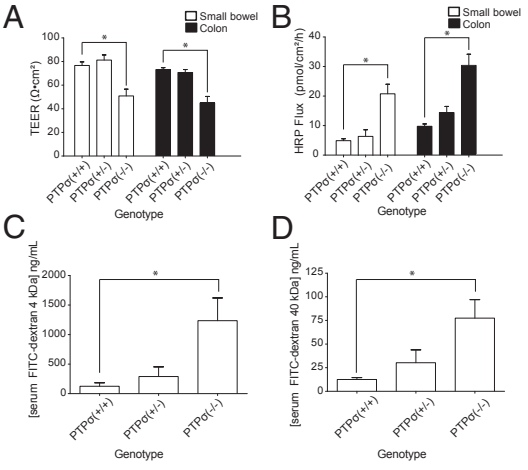

Fig. 1. PTPσ$^{-/-}$ mice exhibit defects in epithelial barrier permeability. (*A*) Transepithelial electrical resistance (TEER) was measured ex vivo in whole intestinal tissue sections mounted in an Ussing chamber. PTPσ$^{-/-}$ mice showed decreased resistance in both the small bowel and colon compared with WT littermates. (*B*) Macromolecular flux across the epithelia was evaluated by adding HRP as a tracer to the mucosal side of the Ussing chamber with tissues mounted. Measurement of the concentration of HRP in the serosal chambers at 30-min intervals revealed an increased flux in the PTPσ$^{-/-}$ mice compared with WT littermates. (*C*) To evaluate permeability in vivo, PTPσ$^{-/-}$ mice and controls were orogastrically gavaged with the molecular tracer FITC–dextran. PTPσ$^{-/-}$ mice showed increased serum levels of FITC–dextran 4 kDa compared with WT littermates. (*D*) PTPσ$^{-/-}$ mice showed increased serum levels of FITC–dextran 40 kDa compared with WT littermates. Data represent means ± SD (*$P < 0.05$; $n = 7$–9 mice per genotype; Student *t* test).

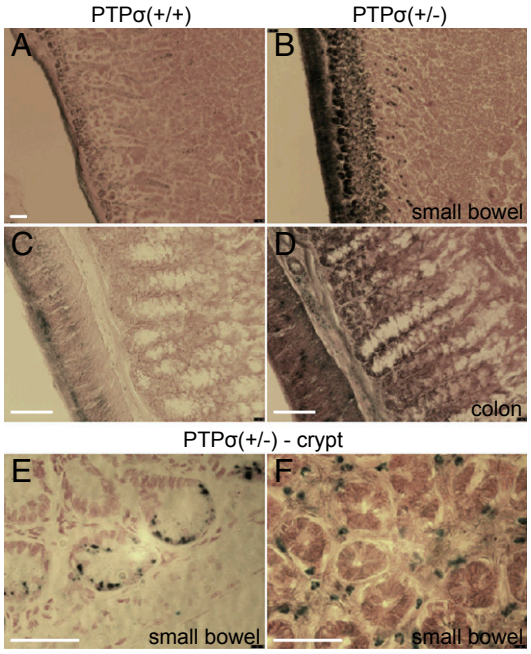

Fig. 2. PTPσ (*PTPRS*) is expressed in cells lining the crypts of the mouse small bowel and colon. X-gal staining, representing *PTPRS* expression (black/dark brown), was performed on frozen-tissue sections from PTPσ$^{+/+}$ and PTPσ$^{+/-}$ mice. (*A* and *B*) X-gal staining was observed in the epithelial cells lining the base of the crypts of the small bowel of PTPσ$^{+/-}$ mice. (*C*) Higher-magnification image demonstrating X-gal staining at the base of the intestinal crypts. (*D* and *E*) X-gal staining was present in the epithelial cells lining the crypts in the colon of the PTPσ$^{+/-}$ mice but not in WT controls. (*F*) High-magnification image of crypts cross-section of PTPσ$^{+/-}$ mouse small bowel demonstrating X-gal–positive cells in the lamina propria region. (Scale bars: 25 μm.)

increased FITC serum levels for both dextran conjugates compared with PTPσ$^{+/+}$ littermates (Fig. 1 *C* and *D*). PTPσ$^{+/-}$ mouse tissue showed slightly elevated levels but were not significantly different from their PTPσ$^{+/+}$ littermates. These data support the Ussing chamber results and further suggest a role for PTPσ in the maintenance of epithelial barrier integrity.

***PTPRS* Is Expressed in the Crypts Regions of Mouse Intestine.** The gene-inactivating cassette used to generate our PTPσ$^{-/-}$ mice contains a β-galactosidase reporter, which is thus expressed from the endogenous *PTPRS* promoter (11). To determine where *PTPRS* (PTPσ) is expressed in the intestine, we performed X-gal staining on frozen tissue sections from PTPσ$^{+/-}$ mice. Dark blue/black staining indicative of PTPσ expression was observed in the epithelial cells lining the crypt region of the small bowel and colon in the heterozygous mice that was not present in the WT (Fig. 2). In the small bowel, PTPσ expression appeared most prominent at the base of the crypts (Fig. 2*C*), an area of rapid cell proliferation. In addition, we also observed PTPσ expression in cells present in the lamina propria regions of the small bowel and colon (Fig. 2 *B* and *E*), including macrophages and lymphocytes (Fig. S1).

Enriched Tyr Phosphorylation in the Crypts of PTPσ$^{-/-}$ Mouse Colon and Small Bowel. To determine how loss of PTPσ regulation affects Tyr phosphorylation in the intestine, we investigated the localization and extent of Tyr phosphorylation in PTPσ$^{-/-}$ and PTPσ$^{+/+}$ mouse colon and small bowel using immunofluorescence microscopy. Colon and small bowel sections from both untreated and DSS-treated PTPσ$^{+/+}$ and PTPσ$^{-/-}$ mice were immunostained using anti-phosphotyrosine (pTyr) antibody (Fig. 3). In the untreated mice, the villi in the small bowel did not show significant pTyr staining in either the PTPσ$^{+/+}$ or PTPσ$^{-/-}$

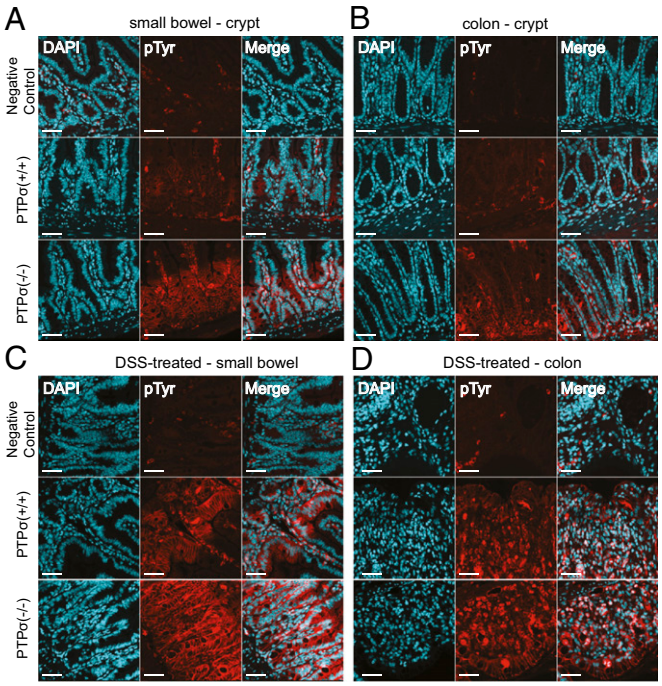

Fig. 3. Tyr phosphorylation is enriched in the crypt regions of PTPσ$^{-/-}$ mouse colon and small bowel. Tissue sections from both naïve and DSS-treated mice were immunostained with anti-pTyr antibody and visualized using confocal microscopy. (*A*) Tyr phosphorylation is enriched in the crypt region of PTPσ$^{-/-}$ mouse small bowel compared with littermate controls. Increased Tyr phosphorylation is also observed in cells contained within the lamina propria regions of PTPσ$^{-/-}$ mice. (*B*) Increased Tyr phosphorylation is visible in the crypt regions of the colon in PTPσ$^{-/-}$ mice compared with littermate controls. (*C* and *D*) DSS treatment of the PTPσ$^{-/-}$ mice and littermates leads to increased Tyr phosphorylation in both KO and WT small bowel (*C*) and colonic (*D*) tissues. (Scale bars: 25 μm.)

sections. In contrast, the crypt regions of the PTPσ$^{-/-}$ small bowel showed strong pTyr staining compared with PTPσ$^{+/+}$ controls (Fig. 3*A*). A similar crypt staining pattern was also observed in the colon of PTPσ$^{-/-}$ mice (Fig. 3*B*). Interestingly, this Tyr phosphorylation pattern colocalized with the AJC marker E-cadherin (Fig. S2). In addition, cells in the lamina propria along the crypt–villus axis showed increased Tyr phosphorylation in the PTPσ$^{-/-}$ mice (Fig. 3*A*). These results support the X-gal staining (Fig. 2), because the increase in Tyr phosphorylation is located in regions positive for PTPσ expression.

In the DSS-treated mice, pTyr staining was enriched in all genotypes in both the small bowel (Fig. 3*C*) and colon (Fig. 3*D*), with further increase in the PTPσ$^{-/-}$ mice relative to DSS-treated control littermates.

Identification of Ezrin and Villin as Binding Partners for PTPσ. The increased permeability and Tyr phosphorylation in the PTPσ$^{-/-}$ mouse intestine suggest that PTPσ is regulating proteins associated with maintenance of the epithelial barrier. To identify the intestinal substrates of PTPσ that may regulate intestinal barrier integrity, we performed mass spectrometry (MS) on colon homogenates from PTPσ$^{-/-}$ and PTPσ$^{+/+}$ mice following immunoprecipitation (IP) with anti-pTyr antibodies and trypsin digestion, to identify hyper–Tyr-phosphorylated proteins in the knockout (KO) colons. Table S1 reveals 37 proteins enriched in Tyr phosphorylation in the PTPσ$^{-/-}$ colon relative to WT, with some of them (e.g., E-Cadherin, β-catenin, p130CAS, EGFR) already identified earlier as PTPσ substrates (15, 32, 33). Among the new putative substrates, we noticed numerous AJC proteins, including ezrin and villin (Table S1). Ezrin is implicated in the organization of the apical web region and participates in several signaling pathways including adherens junction remodeling (34, 35), and Ezr$^{-/-}$ mice have defects in intestinal epithelial architecture (31). Villin regulates actin filaments, cell morphology, and microvilli formation (36), and loss of villin increases colonic susceptibility to the DSS model of murine colitis (36).

To confirm the MS data, an in vitro substrate-trapping assay was performed using GST-fusion proteins that contain the catalytically active D1 domain of PTPσ or its inactive, substrate-trapping PTPσD1(D1472A) mutant (14). Fig. 4 *A* and *B* shows that ezrin and villin can bind to the D1 domain of PTPσ but not to GST alone.

Ezrin Is a Substrate of PTPσ. To test whether ezrin and villin are substrates of PTPσ, an in vitro dephosphorylation assay was performed. GST-fusion proteins containing the intracellular PTPase domains of PTPσ were purified, and their phosphatase activity was determined by incubation with *para*-nitrophenyl phosphate (pNPP), a generic pTyr substrate (Fig. 4*C*). Only fusion proteins containing the active D1 domain (PTPσD1 and PTPσD1D2) showed PTPase activity. The PTPσD1(D1472A) mutant showed no activity, as expected. To test for dephosphorylation of ezrin in cell lysate, purified GST-tagged PTPσD1, PTPσD1D2, or the inactive PTPσD2 and PTPσD1 (D1472A) were incubated with immunoprecipitated FLAG–ezrin and immunoblotted for anti-pTyr. Fig. 4 *E* and *F* reveal significantly decreased Tyr phosphorylation of ezrin in those incubations containing the catalytically active domain of PTPσ but not with the inactive domains. Ezrin binding to and dephosphorylation by PTPσ were lost by pervanadate (a PTP inhibitor) treatment (Fig. S3). No change in Tyr phosphorylation of villin was observed (Fig. 4*D*), suggesting that villin is not an in vitro (direct) substrate of PTPσ (although we cannot preclude the possibility that in vivo PTPσ may indirectly dephosphorylate villin).

Ezrin Localization Is Altered by PTPσ-Mediated Tyr Dephosphorylation in Cells and in the Small Bowel of DSS-Treated Mice. Tyr phosphorylation has been implicated in ezrin trafficking to the PM (37, 38). In accordance, we found that treatment of cells with pervanadate led to accumulation of ezrin at the PM (Fig. 5*A*), suggesting that its Tyr phosphorylation is required for this PM localization.

Phosphorylation of tyrosines Y145, Y191, Y353, and Y477 in ezrin was previously described and has been implicated in a range of processes, including cellular adhesion (35) and cytoskeletal remodeling (39). Thus, we mutated each of these tyrosines to either Phe or the phosphomimetic Glu, transfected them into colonic Caco-2 cells, and followed ezrin distribution by confocal microscopy. As seen in Fig. 5*A* and quantified in Fig. 5*B*, there was a significant redistribution of two ezrin mutations (Y145 and Y353E) from the cytoplasm to the cell periphery relative to the Y145F or Y353F mutant, respectively. The other mutants did not exhibit altered distribution. MS analysis of pervanadate-pretreated ezrin following incubation with the active domain of PTPσ revealed decreased abundance of phosphopeptides containing pY353, indicative of tyrosine phosphatase activity directed toward this site (Fig. 5 *C* and *D*). Moreover, the relative distribution of Tyr-phosphorylated peptides determined by our MS analysis of the PTPσ KO colons demonstrated greater phosphorylation of Y145 and Y353 relative to other pTyr sites (Fig. S4). These results suggest that Y353 and Y145 are likely important tyrosines that are normally dephosphorylated by PTPσ, leading to redistribution of ezrin in the cell. This dephosphorylation-dependent cytoplasmic redistribution is likely not mediated by E-cadherin since although ezrin can (weakly) bind E-cadherin, this interaction is diminished, not increased, in the ezrin-Y353E mutant (Fig. S5).

To complement the ezrin localization experiments, we performed immunofluorescence analysis on mouse tissue sections from our PTPσ$^{-/-}$ and PTPσ$^{+/+}$ mice. Small bowel and colonic tissue was acquired from both naïve and DSS-treated PTPσ$^{-/-}$

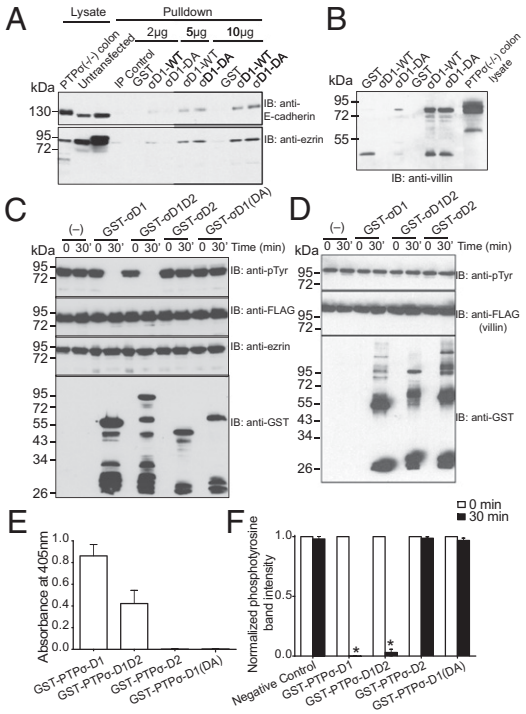

Fig. 4. Ezrin and villin bind the D1 domain of PTPσ and ezrin is a PTPσ substrate. Lysates obtained from PTPσ$^{-/-}$ intestines were incubated with WT (GST-PTPσD1-WT) or substrate-trapping [GST-PTPσD1(D1472A)] mutant bound to GST–agarose containing the catalytic D1 domain of PTPσ. Binding partners were separated on SDS/PAGE and immunoblotted as indicated. (*A*) Substrate-trapping assay revealing ezrin binding to the D1 domain of PTPσ. E-cadherin was included as a positive control. GST alone served as a negative control. IP control is TTC7A, an unrelated protein that is not expressed in the AJC. (*B*) Substrate-trapping assay, revealing villin binding to the D1 domain of PTPσ. σD1-WT and σD1-DA refer to GST-PTPσD1-WT and GST-PTPσD2 (D1472A), respectively. (*C*) Incubation with GST-PTPσD1 or GST-PTPσD1D2 leads to decreased Tyr phosphorylation of FLAG–ezrin. No change in Tyr phosphorylation was observed upon incubations with GST-PTPσD2 or GST-PTPσD1(D1472A). (*D*) Villin is not dephosphorylated by PTPσ in vitro. (*E*) GST-fusion proteins of the indicated PTPσ constructs were incubated with pNPP and phosphatase assay performed to determine catalytic activity. (*F*) Quantification of four experiments similar to that shown in *C*. Data are means ± SD (*$P < 0.05$; $n = 4$; Student *t* test).

and PTPσ$^{+/+}$ mice. Ezrin localization in naïve mouse colon and small bowel revealed no difference between PTPσ$^{-/-}$ and PTPσ$^{+/+}$ sections (Fig. 6*A*). However, differences in ezrin localization were observed between PTPσ$^{-/-}$ and PTPσ$^{+/+}$ small bowel sections after DSS treatment (Fig. 6*B*). The PTPσ$^{+/+}$ small bowel tissue showed ezrin localization in both the cytoplasm and at the PM, in contrast to the PTPσ$^{-/-}$ tissue, which showed PM staining almost exclusively (and in line with our observations in Fig. 5). This suggests that PTPσ may regulate ezrin trafficking and that loss of PTPσ leads to accumulation of ezrin at the PM under acute inflammatory conditions.

Discussion

We demonstrate here a defect in intestinal barrier integrity of the PTPσ$^{-/-}$ mice, suggesting destabilized epithelial monolayer that forms the barrier between the intestinal lumen and lamina propria. Cell adhesion, mediated by the AJC, is essential to barrier function of polarized epithelia (30). Interestingly, our MS analysis identified numerous hyper–Tyr-phosphorylated proteins in the PTPσ$^{-/-}$ mouse intestine with functions associated with the AJC. These hits include proteins that mediate intercellular junctioning (E-cadherin, β-catenin, Tjp-2), proteins that regulate interactions with the actin cytoskeleton (villin, ezrin, gelsolin), and proteins that regulate signaling pathways that modulate junction complex formation and remodeling (EGFR, ezrin). We postulate that PTPσ functions as a positive regulator of epithelial barrier integrity in the intestine through the regulation of

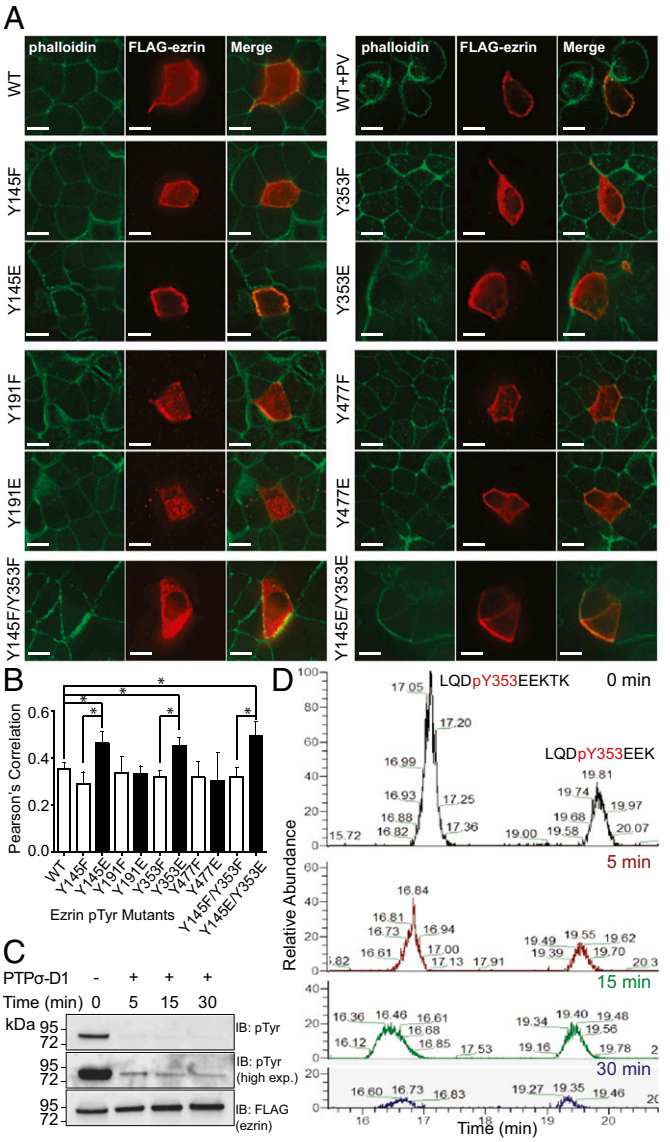

Fig. 5. Ezrin Y145E and Y353E exhibit increased localization at the PM in Caco-2 cell monolayers. FLAG–ezrin (WT or pTyr mutants) was transfected into Caco-2 cells, seeded on Transwell permeable supports, and analyzed by immunofluorescence microscopy to evaluate subcellular localization. (*A*) Localization of ezrin-Y353E, ezrin-Y145E, and the double-mutant ezrin-Y145E/Y353E appears elevated at the PM compared with WT and corresponding Phe mutants. (Scale bars: 10 μm.) (*B*) Colocalization of ezrin with F-actin, as stained by phalloidin, was quantitated using Volocity to determine the degree of correlation. Ezrin-Y145E, -Y353E, and -Y145E/Y353E each showed statistically significant increases in colocalization with actin compared with both WT and the corresponding Phe mutants. Data represent means ± SD (*$P < 0.05$; Student *t* test; $n = 50$–60 cells). (*C*) In vitro dephosphorylation assay conducted on pervanadate-treated WT FLAG–ezrin protein using the GST-fusion protein containing the D1 domain of PTPσ. Each reaction was incubated for the time points listed. Ezrin protein in these reactions was analyzed using MS to identify site-specific changes in Tyr phosphorylation. (*D*) Mass chromatograms for each time point in *C*, demonstrating a decrease in the relative abundance of the phosphopeptides LQDpYEEKTK and LQDpYEEK (which include Y353) with time, indicative of dephosphorylation by PTPσ.

proteins associated with the AJC, including ezrin. Although E-cadherin and β-catenin form the essential core of the adherens junction, and we previously demonstrated these proteins to be colonic PTPσ substrates (15), we believe that PTPσ-mediated regulation of ezrin is another mode in which this PTP regulates the AJC, likely independent of E-cadherin (Fig. S5).

We demonstrate that ezrin is a direct intestinal substrate of PTPσ and that its cellular localization is altered by Tyr dephosphorylation of ezrin-Y353/Y145 by PTPσ, indicating that Tyr phosphorylation of ezrin, especially at Y353 or Y145, is required to localize/maintain it at the PM. Interestingly, DSS treatment, used to induce colitis, augments the PM localization of ezrin in the PTPσ$^{-/-}$ mice, suggesting that DSS or colitis may increase Tyr phosphorylation of ezrin, leading to its increased retention (or arrival) at the PM. The presence of this mislocalization mainly during DSS-treatment does suggest that other PTPs are likely also involved in the regulation of ezrin trafficking, given that we still observe ezrin at the PM in the untreated mice. How Tyr phosphorylation of ezrin regulates its cellular localization in not known, but its phosphorylation is essential for its function as a scaffold protein. In accordance, several binding partners of ezrin, including Src [which phosphorylates Y145 and Y477 (40)] and p85 [the regulatory subunit of PI3K, which is recruited to pY353 (41)], bind to it through SH2 domain-mediated interactions. PTPσ could potentially regulate the ezrin-mediated activation of these effectors by targeting pTyr residues that serve as SH2-binding sites. Interestingly, several of the signaling pathways regulated by ezrin are important for cell adhesion. Rac1 is a potent regulator of actin cytoskeletal dynamics and was shown to regulate adherens junction assembly through E-cadherin (35). In addition, Src is a known mediator of cell adhesion and adherens junction remodeling (40).

In the context of IBD pathogenesis, it is possible that the defective barrier integrity observed the PTPσ$^{-/-}$ mouse intestine may contribute to the development of intestinal enteropathies by increasing the exposure of the lamina propria to luminal pathogens. A "leaky" intestinal epithelium has been previously implicated in IBD (30) and barrier defects have been observed in IBD patients (42), but the underlying genetic basis for these effects were not well characterized. Our work presented here suggests a new function for PTPσ as a positive regulator of epithelial barrier integrity, which may help explain the underlying genetic risk in IBD associated with defects in permeability. Our current work, however, cannot preclude the possibility that cells in the lamina propria (such as macrophages or lymphocytes), which express PTPσ, also contribute to the intestinal pathogenesis we observe in the PTPσ$^{-/-}$ mice.

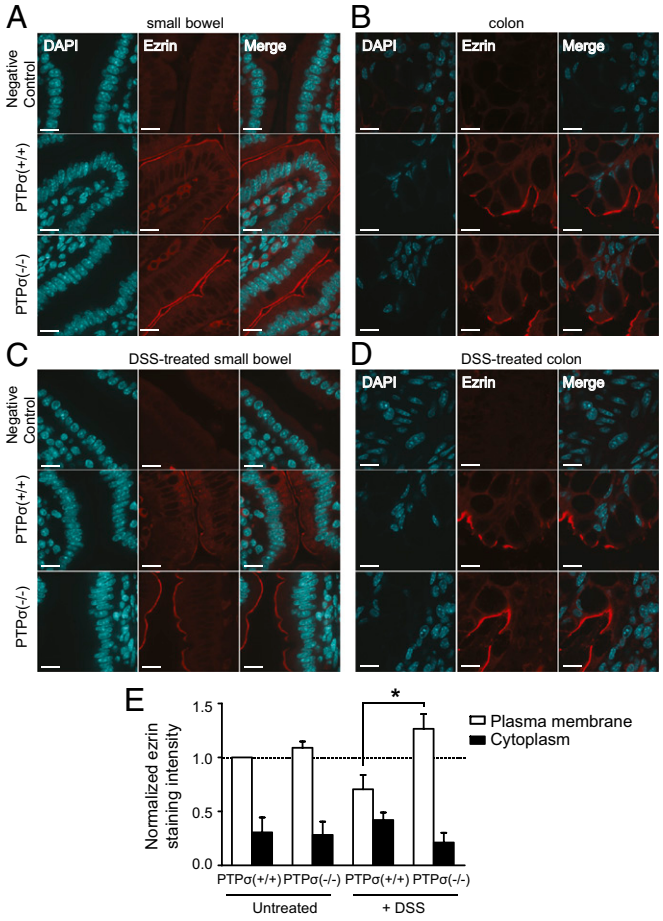

Fig. 6. Ezrin localization is altered in the small bowel of PTPσ$^{-/-}$ mice after colitis-inducing DSS treatment. Ezrin localization was evaluated in small bowel and colon tissue sections from both naïve and DSS-treated PTPσ$^{-/-}$ mice and littermate controls using immunofluorescence microscopy. (*A*) Ezrin present at the apical PM of enterocytes in the small bowel in PTPσ$^{-/-}$ mice and controls. (*B*) Ezrin localizes to the apical surface of enterocytes in the colon, but there was no observed difference between PTPσ$^{-/-}$ mice and littermate controls. (*C*) Ezrin localization is disrupted in the small bowel of PTPσ$^{-/-}$ mice treated with DSS. (*D*) DSS treatment has no effect on the localization of ezrin in the colon. (Scale bars: 25 μm.) (*E*) Quantification of ezrin-staining intensity in enterocytes of both naïve and DSS treated PTPσ$^{+/+}$ and PTPσ$^{-/-}$ mice. All staining-intensity values were normalized to the mean PM intensity observed in the naïve PTPσ$^{+/+}$ mice. Images were converted to grayscale, and edges corresponding to the PM were isolated algorithmically. Data are means ± SD (n = 40–50 images per genotype; *P = 0.0046; Student t test).

Materials and Methods

Generation of Constructs and pTyr Mutants. FLAG epitope-tagged full-length ezrin- and villin-fusion constructs were generated as described in *SI Materials and Methods*. Site-directed mutagenesis was performed to generate phosphomimetic (Y→E) and phosphoablated (Y→F) ezrin mutants at sites Y145, Y191, Y353, and Y477 (Table S2).

Tandem Immunoprecipitation of pTyr–MS. pTyr-containing proteins were isolated from PTPσ$^{-/-}$ and WT littermate intestinal tissue homogenates by IP, digested with trypsin to generate peptide fragments, and characterized through tandem MS as outlined in *SI Materials and Methods*. Identified proteins were ranked according to the difference in unique spectral counts between the PTPσ$^{+/+}$ and PTPσ$^{-/-}$ mice.

In Vitro Substrate-Trapping and Dephosphorylation Assays. GST-fusion proteins containing the intracellular PTPase domains of PTPσ (14), including a substrate-trapping D1472A mutant, were used to immunoprecipitate FLAG-tagged ezrin- and villin-fusion proteins as described in *SI Materials and Methods*. Dephosphorylation assays were performed in vitro using these GST-fusion proteins.

Ussing Chamber Studies. PTPσ$^{-/-}$, PTPσ$^{+/-}$, and WT littermates were killed by cervical dislocation; small bowel (proximal to cecum) and colonic (proximal to rectum) sections were excised and mounted in an Ussing chamber as detailed in *SI Materials and Methods*. Macromolecular flux was assessed by the addition of unconjugated horseradish peroxidase (HRP) to the luminal chamber as described (43).

FITC–Dextran Assay. PTPσ$^{-/-}$, PTPσ$^{+/-}$, and WT littermates were orogastrically gavaged with FITC–dextran (4 and 40 kDa). After 4 h, mice were killed by cervical dislocation, blood was extracted by cardiac puncture and then separated by centrifugation, and serum levels of FITC were analyzed by fluorimetry as detailed in *SI Materials and Methods*.

Immunohistochemistry. Small bowel and colonic tissue from PTPσ$^{-/-}$ mice and WT littermates were embedded in paraffin, sectioned (5 μm), processed, and immunostained with anti–E-cadherin, anti–β-catenin, and anti-ezrin antibodies as described in *SI Materials and Methods*.

Immunofluorescence Microscopy on Caco-2 Monolayers. Caco-2 BBe cells were transiently transfected in suspension with FLAG-tagged WT or pTyr mutant ezrin. Transfected cells were seeded onto Transwell permeable supports and grown for 4 d as outlined in *SI Materials and Methods*. Membranes containing cell monolayers were mounted on glass slides for immunofluorescence microscopy using anti-FLAG antibodies and Alexa Fluor 488-conjugated phalloidin.

Identification of pTyr Sites by MS. WT FLAG–ezrin was transiently transfected in HEK293T cells. Following pervandate treatment to enrich for Tyr phosphorylation, ezrin was immunoprecipitated and incubated with the D1 domain of PTPσ for various time points as described in *SI Materials and Methods*. The bound FLAG–ezrin was digested with trypsin, and the resulting pTyr-containing peptide fragments were isolated by IP then analyzed by MS (as above).

ACKNOWLEDGMENTS. We thank A. Aizic, M. Gareau, W. Glowacka, C. Jiang, C. Lu, and R. Fattouh for technical support. This work was supported by Canadian Institute of Health Research Grants FRN 86496 (to D.R.) and MOP119457 (to A.M.). D.R. holds a Canada Research Chair (Tier I) from the Canadian Foundation for Innovation, and A.M. is supported by an Early Researcher Award from the Ontario Ministry of Research and Innovation.

1. Alonso A, et al. (2004) Protein tyrosine phosphatases in the human genome. *Cell* 117(6):699–711.
2. Pulido R, Serra-Pagès C, Tang M, Streuli M (1995) The LAR/PTP delta/PTP sigma subfamily of transmembrane protein-tyrosine-phosphatases: Multiple human LAR, PTP delta, and PTP sigma isoforms are expressed in a tissue-specific manner and associate with the LAR-interacting protein LIP.1. *Proc Natl Acad Sci USA* 92(25):11686–11690.
3. Wang H, et al. (1995) Expression of receptor protein tyrosine phosphatase-sigma (RPTP-sigma) in the nervous system of the developing and adult rat. *J Neurosci Res* 41(3):297–310.
4. Kim H, et al. (1996) Expression of LAR-PTP2 in rat lung is confined to proliferating epithelia lining the airways and air sacs. *Am J Physiol* 270(4 Pt 1):L566–L576.
5. McLean J, Batt J, Doering LC, Rotin D, Bain JR (2002) Enhanced rate of nerve regeneration and directional errors after sciatic nerve injury in receptor protein tyrosine phosphatase sigma knock-out mice. *J Neurosci* 22(13):5481–5491.
6. Thompson KM, et al. (2003) Receptor protein tyrosine phosphatase sigma inhibits axonal regeneration and the rate of axon extension. *Mol Cell Neurosci* 23(4):681–692.
7. Sapieha PS, et al. (2005) Receptor protein tyrosine phosphatase sigma inhibits axon regrowth in the adult injured CNS. *Mol Cell Neurosci* 28(4):625–635.
8. Fry EJ, Chagnon MJ, López-Vales R, Tremblay ML, David S (2010) Corticospinal tract regeneration after spinal cord injury in receptor protein tyrosine phosphatase sigma deficient mice. *Glia* 58(4):423–433.
9. Shen Y, et al. (2009) PTPsigma is a receptor for chondroitin sulfate proteoglycan, an inhibitor of neural regeneration. *Science* 326(5952):592–596.
10. Martin KR, et al. (2011) Identification of PTPsigma as an autophagic phosphatase. *J Cell Sci* 124(Pt 5):812–819.
11. Wallace MJ, et al. (1999) Neuronal defects and posterior pituitary hypoplasia in mice lacking the receptor tyrosine phosphatase PTPsigma. *Nat Genet* 21(3):334–338.
12. Elchebly M, et al. (1999) Neuroendocrine dysplasia in mice lacking protein tyrosine phosphatase sigma. *Nat Genet* 21(3):330–333.
13. Meathrel K, Adamek T, Batt J, Rotin D, Doering LC (2002) Protein tyrosine phosphatase sigma-deficient mice show aberrant cytoarchitecture and structural abnormalities in the central nervous system. *J Neurosci Res* 70(1):24–35.
14. Siu R, Fladd C, Rotin D (2007) N-cadherin is an in vivo substrate for protein tyrosine phosphatase sigma (PTPsigma) and participates in PTPsigma-mediated inhibition of axon growth. *Mol Cell Biol* 27(1):208–219.
15. Muise AM, et al. (2007) Protein-tyrosine phosphatase sigma is associated with ulcerative colitis. *Curr Biol* 17(14):1212–1218.
16. Silverberg MS, et al. (2005) Toward an integrated clinical, molecular and serological classification of inflammatory bowel disease: Report of a Working Party of the 2005 Montreal World Congress of Gastroenterology. *Can J Gastroenterol* 19(Suppl A):5–36.
17. Khor B, Gardet A, Xavier RJ (2011) Genetics and pathogenesis of inflammatory bowel disease. *Nature* 474(7351):307–317.
18. Darfeuille-Michaud A, et al. (2004) High prevalence of adherent-invasive Escherichia coli associated with ileal mucosa in Crohn's disease. *Gastroenterology* 127(2):412–421.
19. Swidsinski A, et al. (2002) Mucosal flora in inflammatory bowel disease. *Gastroenterology* 122(1):44–54.
20. Hollander D, et al. (1986) Increased intestinal permeability in patients with Crohn's disease and their relatives. A possible etiologic factor. *Ann Intern Med* 105(6): 883–885.
21. Roth MP, et al. (1989) Familial empiric risk estimates of inflammatory bowel disease in Ashkenazi Jews. *Gastroenterology* 96(4):1016–1020.
22. Tysk C, Lindberg E, Järnerot G, Flodérus-Myrhed B (1988) Ulcerative colitis and Crohn's disease in an unselected population of monozygotic and dizygotic twins. A study of heritability and the influence of smoking. *Gut* 29(7):990–996.
23. Wolters VM, et al. (2011) Replication of genetic variation in the MYO9B gene in Crohn's disease. *Hum Immunol* 72(7):592–597.
24. Wapenaar MC, et al. (2008) Associations with tight junction genes PARD3 and MAGI2 in Dutch patients point to a common barrier defect for coeliac disease and ulcerative colitis. *Gut* 57(4):463–467.
25. Muise AM, et al. (2009) Polymorphisms in E-cadherin (CDH1) result in a mis-localised cytoplasmic protein that is associated with Crohn's disease. *Gut* 58(8):1121–1127.
26. Barrett JC, et al.; UK IBD Genetics Consortium; Wellcome Trust Case Control Consortium 2 (2009) Genome-wide association study of ulcerative colitis identifies three new susceptibility loci, including the HNF4A region. *Nat Genet* 41(12):1330–1334.
27. Lee S, et al. (2007) Dimerization of protein tyrosine phosphatase sigma governs both ligand binding and isoform specificity. *Mol Cell Biol* 27(5):1795–1808.
28. Franke A, et al. (2010) Genome-wide meta-analysis increases to 71 the number of confirmed Crohn's disease susceptibility loci. *Nat Genet* 42(12):1118–1125.
29. Jostins L, et al.; International IBD Genetics Consortium (IIBDGC) (2012) Host-microbe interactions have shaped the genetic architecture of inflammatory bowel disease. *Nature* 491(7422):119–124.
30. Laukoetter MG, Bruewer M, Nusrat A (2006) Regulation of the intestinal epithelial barrier by the apical junctional complex. *Curr Opin Gastroenterol* 22(2):85–89.
31. Saotome I, Curto M, McClatchey AI (2004) Ezrin is essential for epithelial organization and villus morphogenesis in the developing intestine. *Dev Cell* 6(6):855–864.
32. Chagnon MJ, et al. (2010) Receptor tyrosine phosphatase sigma (RPTPσ) regulates, p250GAP, a novel substrate that attenuates Rac signaling. *Cell Signal* 22(11): 1626–1633.
33. Vijayvargia R, Kaur S, Krishnasastry MV (2004) alpha-Hemolysin-induced dephosphorylation of EGF receptor of A431 cells is carried out by rPTPsigma. *Biochem Biophys Res Commun* 325(1):344–352.
34. Hiscox S, Jiang WG (1999) Ezrin regulates cell-cell and cell-matrix adhesion, a possible role with E-cadherin/beta-catenin. *J Cell Sci* 112(Pt 18):3081–3090.
35. Pujuguet P, Del Maestro L, Gautreau A, Louvard D, Arpin M (2003) Ezrin regulates E-cadherin-dependent adherens junction assembly through Rac1 activation. *Mol Biol Cell* 14(5):2181–2191.
36. Wang Y, et al. (2008) A novel role for villin in intestinal epithelial cell survival and homeostasis. *J Biol Chem* 283(14):9454–9464.
37. Wu YX, Uezato T, Fujita M (2000) Tyrosine phosphorylation and cellular redistribution of ezrin in MDCK cells treated with pervanadate. *J Cell Biochem* 79(2):311–321.
38. Jiang WG, et al. (1995) Induction of tyrosine phosphorylation and translocation of ezrin by hepatocyte growth factor/scatter factor. *Biochem Biophys Res Commun* 217(3):1062–1069.
39. Coffey GP, et al. (2009) Engagement of CD81 induces ezrin tyrosine phosphorylation and its cellular redistribution with filamentous actin. *J Cell Sci* 122(Pt 17):3137–3144.
40. Srivastava J, Elliott BE, Louvard D, Arpin M (2005) Src-dependent ezrin phosphorylation in adhesion-mediated signaling. *Mol Biol Cell* 16(3):1481–1490.
41. Gautreau A, Poullet P, Louvard D, Arpin M (1999) Ezrin, a plasma membrane-microfilament linker, signals cell survival through the phosphatidylinositol 3-kinase/Akt pathway. *Proc Natl Acad Sci USA* 96(13):7300–7305.
42. Mankertz J, Schulzke JD (2007) Altered permeability in inflammatory bowel disease: Pathophysiology and clinical implications. *Curr Opin Gastroenterol* 23(4):379–383.
43. Gareau MG, Jury J, MacQueen G, Sherman PM, Perdue MH (2007) Probiotic treatment of rat pups normalises corticosterone release and ameliorates colonic dysfunction induced by maternal separation. *Gut* 56(11):1522–1528.